
This is an electronic reprint of the original article.
This reprint may differ from the original in pagination and typographic detail.

Machado, Miguel A.; Silva, Maria I.; Martins, Ana P.; Carvalho, Marta S.; Santos, Telmo G.
Double active transient thermography

Published in:
NDT and E International

DOI:
[10.1016/j.ndteint.2021.102566](https://doi.org/10.1016/j.ndteint.2021.102566)

Published: 01/01/2022

Document Version
Peer-reviewed accepted author manuscript, also known as Final accepted manuscript or Post-print

Published under the following license:
CC BY-NC-ND

Please cite the original version:
Machado, M. A., Silva, M. I., Martins, A. P., Carvalho, M. S., & Santos, T. G. (2022). Double active transient thermography. *NDT and E International*, 125, Article 102566. <https://doi.org/10.1016/j.ndteint.2021.102566>

This material is protected by copyright and other intellectual property rights, and duplication or sale of all or part of any of the repository collections is not permitted, except that material may be duplicated by you for your research use or educational purposes in electronic or print form. You must obtain permission for any other use. Electronic or print copies may not be offered, whether for sale or otherwise to anyone who is not an authorised user.

Creative Commons CC-BY-NC-ND

Accepted author manuscript of:

Machado, M.A.; Silva, M.I.; Martins, A.P.; Carvalho, M.S.; Santos, T.G. Double Active Transient Thermography. NDT & E International 2022, v.125, 102566
doi: 10.1016/j.ndteint.2021.102566.

<https://doi.org/10.1016/j.ndteint.2021.102566>

Double Active Transient Thermography

Miguel A. Machado^{a,1}, Maria I. Silva^{a,b}, Ana P. Martins^a, Marta S. Carvalho^a, Telmo G. Santos^a

^aUNIDEMI, Department of Mechanical and Industrial Engineering, NOVA School of Science and Technology, NOVA University Lisbon, 2829-516 Caparica, Portugal.

^bDepartment of Mechanical Engineering, School of Engineering, Aalto University, Puumiehenkuja 3, 02150 Espoo, Finland

¹ Corresponding author: miguel.m@fct.unl.pt

Abstract

This paper presents an innovative variant of the Active Transient Thermography (ATT), designated Double Active Transient Thermography (DATT), where the component inspected is excited by one heat and one cold sources. The goal is to speed up and improve the temperature contrast, namely for polymer matrix composites parts produced by Additive Manufacturing. Finite element analysis of the thermal phenomena involved in DATT were performed to assist the definition of the experimental set-ups and confirm the high potential of the technique.

Experimental results prove that the introduction of the cold flow increases the temperature contrast up to 100%, comparing with ATT, and mid thickness defects are the ones that benefits the most from this technique. Therefore, the improvement of the inspection procedure is achieved by two means: enhancing the thermal contrast of the defects, and/or anticipating the instant when the maximum contrasts occur.

Keywords: Active transient thermography, DATT, Polymer matrix composites, Simulation.

1. Introduction

Over the years, there has been an increased focus on the development of materials, like advanced composites produced by Additive Manufacturing (AM), in order to satisfy industrial and economic requirements, for example, in aerospace and automotive industries, where they seek reduced weight components, with enhanced strength, which improve productivity and fuel economy and reduce CO₂ emissions. This progress raises new demands in characterizing a variety of defects that may appear during its production and service life, which have an impact on the component's performance. Conventional Non-destructive testing (NDT) often cannot fulfil these new requirements, implying the research and development of new, innovative approaches that provide a greater knowledge on how these materials behave, especially in demanding jobs [1,2]. There are currently some challenges, for example, regarding the inspection of composites, including polymer matrix composites, such model complexity [3] and relevant polymers properties, such as low thermal and electrical conductivity [4].

Despite some low conductivity polymeric composite parts may be inspected without contact by eddy currents [5,6], a faster and an image producer NDT technique should be target for such kind of inspections [1,7–9].

The Active Transient Thermography (ATT) can overcome some of the limitations presented so far, which acquires and processes the thermal response of the component when excited by an external thermal source. The thermal energy is usually transmitted by radiation between the specimen and a hot or cold source during a controlled time or by means of a blast of hot air or coolant. In this technique flash tube or bulb is mostly used as the heat source, being almost adopted as a standard procedure with several investigations [10], being the cold source used as thermal excitation in limited cases: when the material to inspect is already at a temperature higher than the ambient temperature or when the specimen under analysis could not be heated [11,12]. Through the temperature contrasts presented in the acquired thermograms, it can be detected and identified superficial and internal defects [13,14]. The presence of discontinuities can be detected because it disrupts the heat flow, due to the variation of the local thermal conductivity of the sample which causes a change in the surface temperature detected by the IR camera [4,14]. Shepard et al. developed a simple model that provides an estimation of signal to background contrast for flash thermography of discrete flat bottom hole type flaws in a solid slab sample. The approach provides real, non-relative, detectability information which can be applied based on estimates of physical properties and camera noise characteristics enhancing the contrast [15].

The constant need to increase the reliability of the inspection has led to the improvement of the inspection parameters and of operational conditions, and to the analysis of the physical phenomena involved, namely, using numerical simulation. Therefore, the cost efficiency and the phenomenological knowledge of the technique is achieved through appropriate numerical modelling [4]. Several authors developed numerical models with commercial finite element codes to predict the detectability of defects [16], estimate the defect size and shape [17], foresee the frame that would best expose the defect [18], identify the most appropriate inspection parameters and optimise the evaluation process [19]. For the numerical models [16,18,20,21], assumptions were used to simplify the computational cost, being the effect of the heat source simulated by applying a uniform heat flux on the flat surface of the specimen that is exposed to the infra-red radiation. For the case of curved panels, a non-uniform heat flux is applied, for which the density distribution must be obtained by experimental testing [20]. To overcome the difficulties regarding the complex geometry of the parts, Carvalho et al. [4] developed a finite element model in ANSYS to solve the heat transient problem which covers the modelling of the radiating surfaces, including the heat source.

Despite recent investigations have been conducted to improve the inspection results by using alternative methods of thermal stimulation including cold [22,23], or improving the image obtained by applying data processing and analysis methods for noise reduction [24,25], when the thermal conductivity of the material is low, as in this case, the contrasts can be reduced and the defects difficult to detect in thickness, especially the deeper ones. Therefore, in this paper, it is presented an innovative variant of the ATT, designated Double Active Transient Thermography (DATT), where the evaluated component is excited by two sources, infrared radiation and a cold flow. The prior advantage of this technique is that, unlike Lock-in Thermography which allows the detection and position of internal defects in thickness, DATT can be a simpler and faster alternative in achieving those similar results, although it depends on the thickness of the sample and needs access to both sides of the sample.

The goal of developing this technique is to speed up and improve the inspection procedure, and to clearly observe, with close temperature contrast, different defects at different depths and locations, as shown in **Fig. 1**. While in ATT the thermography is solely active during the heating phase, being the inspected component passive during its natural cooling, in DATT both heating and cooling phases are active, being a differentiating feature of this technique. Therefore, the improvement of the inspection procedure can be achieved by two means: enhancing the thermal contrast of the defects, mainly those that were harder to identify by ATT, increasing the probability of detection; and/or anticipating the instant when the maximum contrasts occur.

2. Double Active Transient Thermography set-up

2.1. Samples description

As a result of the AM process, defects as voids [26] and poor adhesion of the layers [27] may occur during the material deposition. The test specimen used is a grey Polylactic Acid part produced by material extrusion additive manufacturing, featuring three delaminations, 15 mm square voids created artificially as a feature of the CAD file, depicted in **Fig. 2**. This sample has a wall thickness of 5 mm and a box like shape to prevent the cold source from rapidly escaping the sample.

The delaminations have 0.5 mm thickness and are located at a relative distance of 50 mm from each other, as shown in **Fig. 1**. A second sample was produced, very similar to the boxed one presented but with a few differences. The thickness was changed from 5 mm to 15 mm and only one defect was produced with the same dimensions and was placed in mid thickness (the centre of the defect was 7.5 mm away from both surfaces).

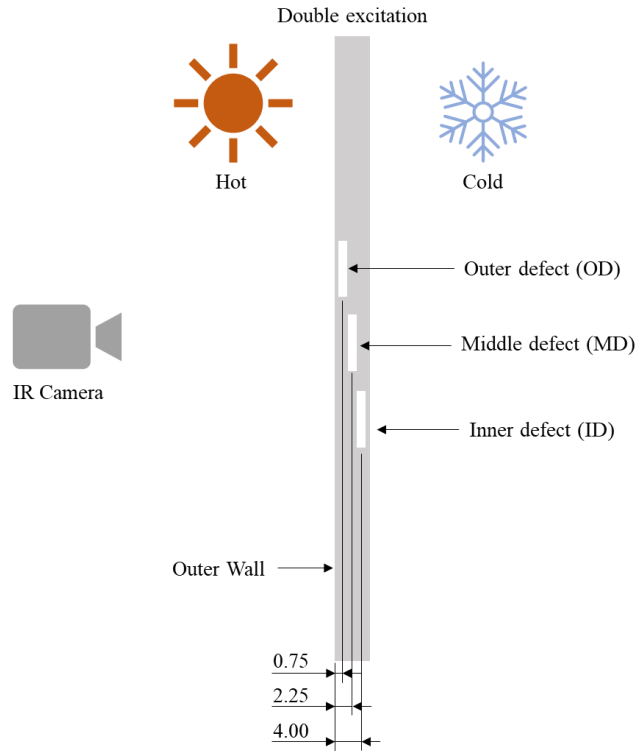


Fig. 1. Schematic representation of the DATT. The specimen has three artificial delaminations defects.

2.2. Experimental set-up

The DATT experimental layout used for inspection is shown in **Fig. 3**. This layout is composed by one heat and one cold sources, one infrared (IR) camera and the test specimen. The hot source and IR camera are located on the plane side of the sample and the cold source is located on the opposite side of the sample.

The hot source consists of four Phillips IR-175C-PAR lamps of 175 W. This group of lamps was placed perpendicular to the test specimen, at a distance of 60 cm, denoted by d_i in the scheme in **Fig. 3**, being also shown in **Fig. 4a** and **Fig. 4c**.

The use of a coolant fluid as a cold source has evident advantages since it has a significant calorific power to insert a cold flow in the sample. This is very useful to demonstrate experimentally the findings of the numerical simulations but, in an industrial setting this may not be possible. The component might react to the liquid or might not be possible to get wet. One solution that possibly overcome this could be the introduction of an air flow at very low temperature.

The IR camera, a Fluke Ti400, to record the thermal response of the sample during its inspection, was placed perpendicular to the plane side of the specimen, at a distance of 80 cm, denoted by d_c in the scheme in **Fig. 3**, and above the lamps, as shown in **Fig. 4a** and **Fig. 4c**.

Software SmartView™ was used in order to collect the temperature points across the thermograms enabling the handling of the data from the inspections.

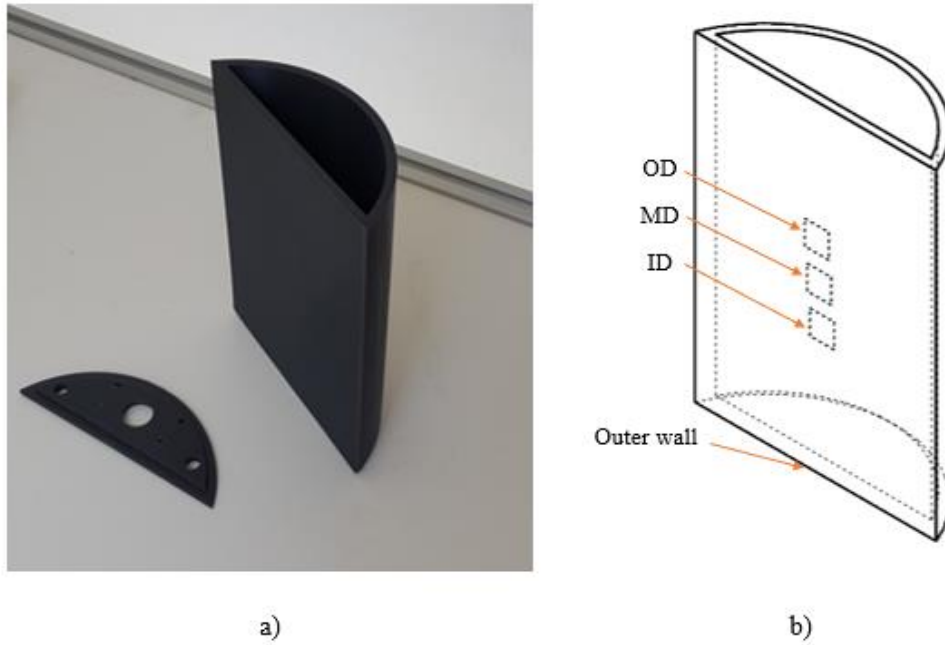


Fig. 2. Sample inspected a) 3D printed version b) model showing the delaminations with the legend of the defects and outer wall.

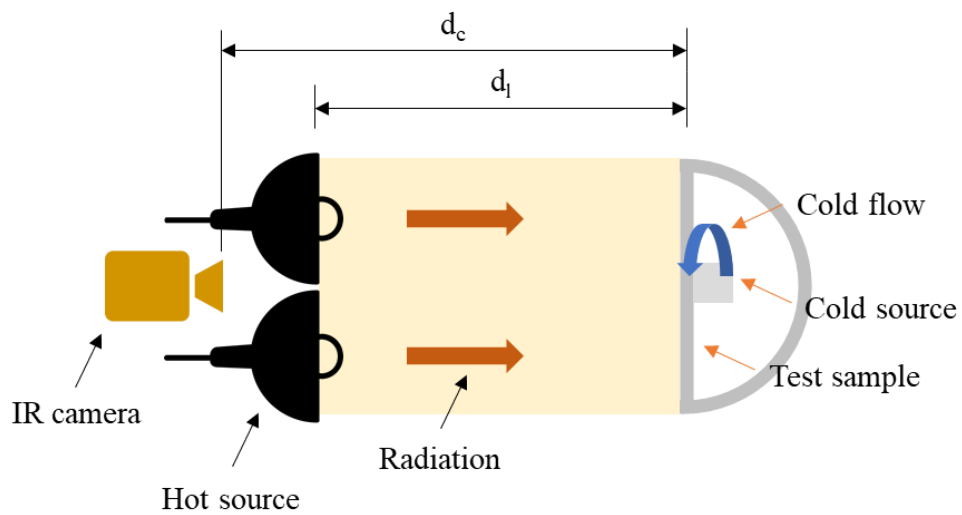


Fig. 3. DATT schematic experiment setup.

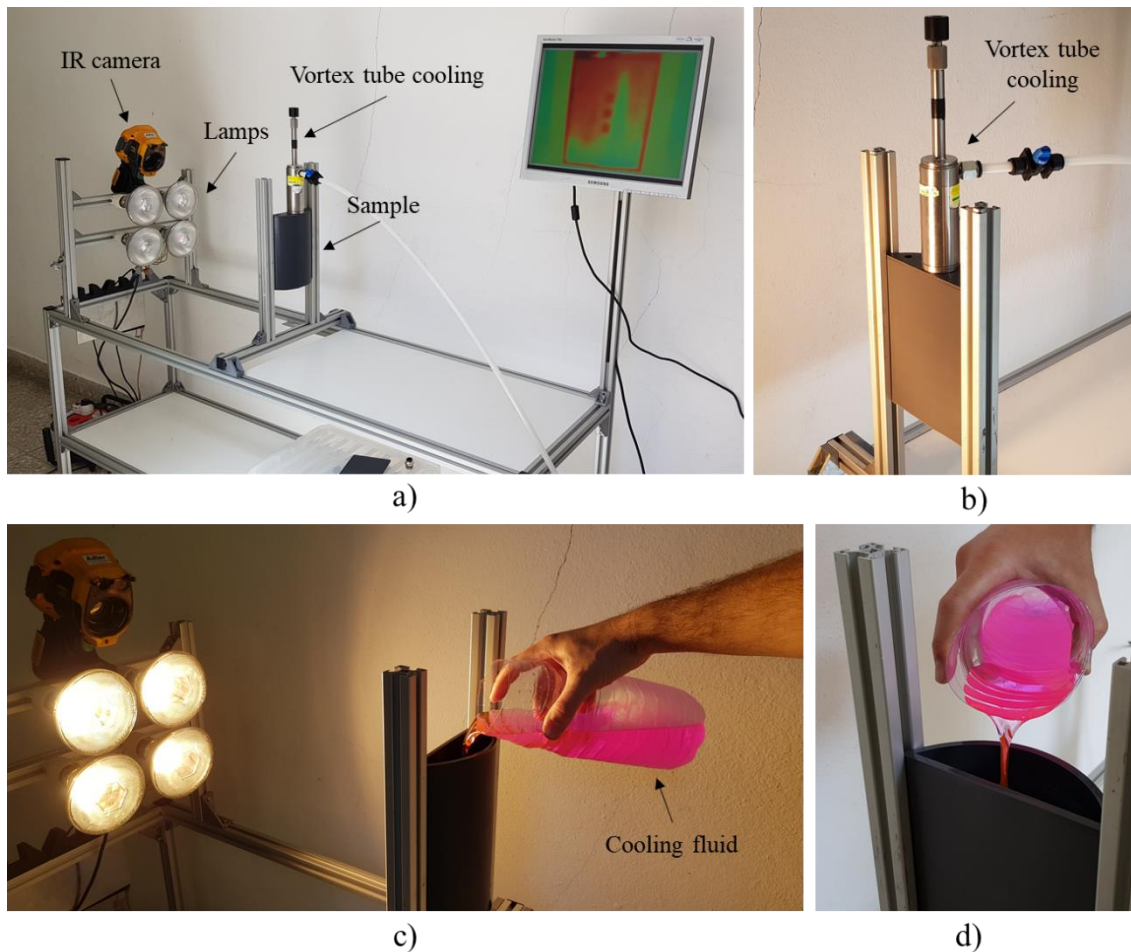


Fig. 4. DATT setup; a) with the vortex; b) vortex tube cooling and sample; c) with the coolant fluid; d) pouring the coolant fluid into the sample.

2.3. Testing procedures

Two sets of experiments were conducted with different cold sources. First, to demonstrate experimentally the findings of the numerical simulations, it was used the coolant fluid which solidifies at $-40\text{ }^{\circ}\text{C}$. The liquid was poured into the sample, as shown in **Fig. 4c** and **Fig. 4d**, taking around 3 s to fill in. With the coolant fluid, the interior of the sample reached around $-20\text{ }^{\circ}\text{C}$. Still, in an industrial setting the use of a coolant fluid may not be possible, and for the second sets of experiments presented here, was used a Meech Vortex Tube to direct the cold air flow. This instrument was placed in the entrance of the lid, above the specimen, perpendicular to it, as shown in **Fig. 4a** and **Fig. 4b**. Beside to place the vortex, the lid was designed also to prevent the cold air from rapidly escaping the sample, and its additional holes reduced the pressure loss in the inlet of the cold flow, as shown in **Fig. 2a**. The air flow of the vortex was around 50 l/min and the interior of the sample reached, on average, $-4\text{ }^{\circ}\text{C}$.

3. Numerical model

For the simulation of the DATT procedure, the commercial code ANSYS was used to calculate the finite element solution. The specimen model is considered to have plane element behaviour and isotropic material properties that do not vary for the analysis temperature range of the NDT procedures. In these simulations, four models meshed with 8 node plane elements were created to represent the geometry of the sections where the defects are located: three sections where the defects appear isolated and one section with the three defects, for which the geometry is represented in the scheme of **Fig. 1**. The material properties for PLA of interest for the purposes of heat transfer simulation are presented in **Table 1**.

Table 1 PLA material properties for the temperature range of the NDT procedures.

Thermal Conductivity [W/m K]	Density [kg/m ³]	Specific heat [J/kg K]
0.13	1240	1800

Being extremely effective in terms of computational cost, the developed model allows to efficiently simulate combinations of parameters, providing an overview of the response of the method under several testing conditions. Therefore, the prescribed boundary conditions for the heated surface is a uniform heat flux of 1500 W/m² applied during 20 s to simulate the income radiation. This approach provides accurate results for flat geometries, for which the computation of the view factors is not significant, and the uniform distribution is an adequate assumption [4]. Similarly, a uniform heat flux of – 10000 W/m² is applied during 20 s on the opposite side to simulate the cooling.

The prescribed initial and boundary conditions were not tuned to be consistent to the corresponding environment conditions of the testing, since these simulations were conducted solely to verify the potential of DATT and to assist the definition of the experimental set-ups. For all the simulations presented here the initial temperature of the entire model was set to 24 °C. Furthermore, the combinations of the heat flows are several for which the simulation of the tests results are presented, although only five cases were then tested for the experimental validation as listed in **Table 2**, for which the heat and cold sources were applied for a limited time, 20 s, in every test.

Table 2 Tests performed for each experiment set.

Test Number	-20 s	-10 s	0 s	10 s	20 s	30 s	40 s
1 Heat only							
2 Heat and cold							
3 Heat then cold							
4 Cold then heat							
5 Cold only							

4. Results and Discussion

4.1. Numerical simulation results

From the point of view of the thermography inspection process, the detection of the defects is visible due to the contrast presented. Therefore, the results of the simulations were taken in two locations, depicted in **Fig. 9**: one point on the outer wall above the defect (DP) and another at half distance between the edge of the defect and the end of the sample (DFP). Mathematically, the contrast is achieved with difference of the temperature between those points.

The simulation results for the three defects contrast are depicted in **Fig. 5**, **Fig. 6** and **Fig. 7**. In these figures, the red curve refers to the contrast obtained when only the hot source was used; the blue curve refers to the contrast obtained when only cold source was used; the black curve refers to the contrast obtained when the hot and cold sources were applied at the same time (Hot and cold); the green curves refer to the contrast obtained when the cold source was used before the hot source (Cold then hot); the pink curves refer to the contrast obtained when the hot source was used before the cold source (Hot then cold).

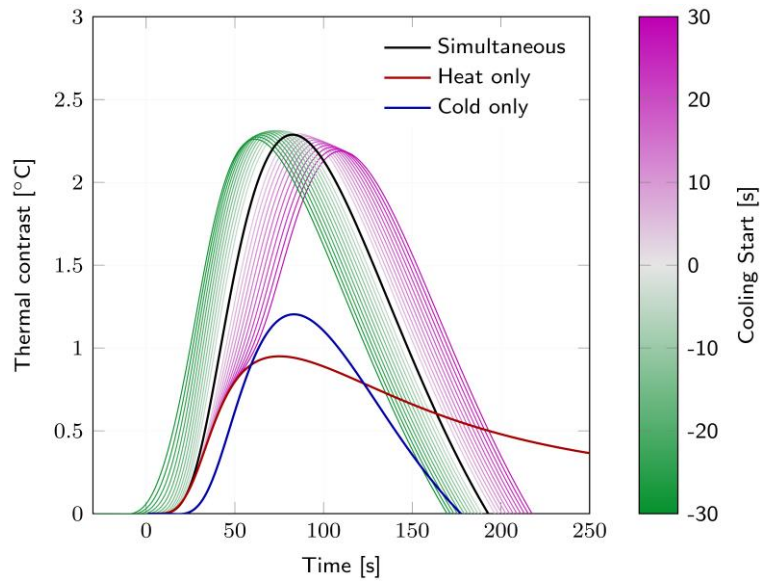


Fig. 5. Simulation results for the mid thickness defect contrast.

Fig. 5 presents the evolution of the thermal contrast in time for the mid thickness defect in three different situations: cold only where the maximum contrast (1.2 °C) occurs at 83 s; using hot and cold simultaneously (DATT), the maximum contrast is 2.3 °C at 83 s, which corresponds to an increase of 141% in the temperature contrast when compared to the use of a heat source, and in 88% when compared to the use of a cold source. The best result can be achieved if the cold source turns on before the hot source. This leads to an anticipation of the maximum thermal contrast by 15 s. The heat path is shorter than half the thickness and there is no resistance (at the interfaces), so the heat wave is reflected faster in the defect. With the cold, the path is longer and there are two resistances/interfaces through the defect, so the time the cold takes to transmit through the defect is greater. The source applied to the surface measured is the one which controls/determines the phenomena, which is clearly seen in **Fig. 6** and **Fig. 7**.

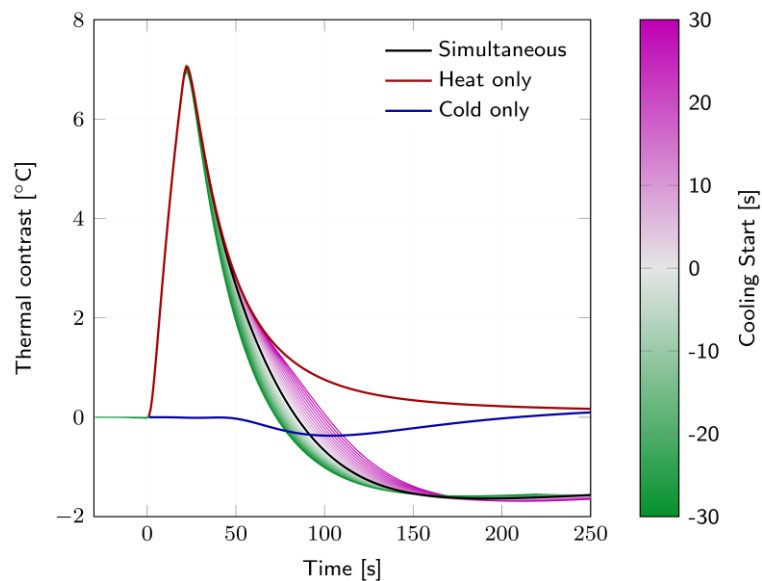


Fig. 6. Simulation results for outer defect contrast.

Simulation results for the outer defect contrast, depicted in **Fig. 6**, suggest that the introduction of the cold flow does not improve the inspection process. However, as shown in **Fig. 7**, the DATT improves the thermal contrast of the inner defect in 20%, when it is compared to the case for which only the cold source is applied and 86% when compared to the heat only case.

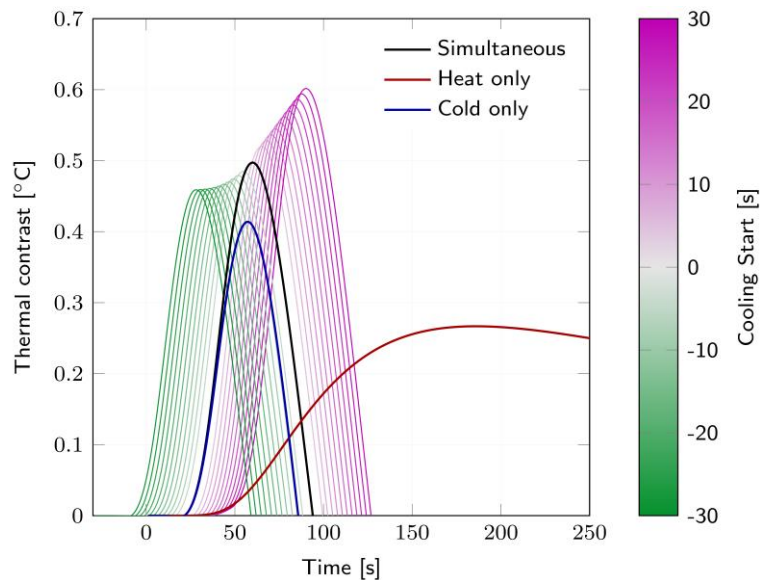


Fig. 7. Simulation results for the inner defect contrast.

For inner defects, the use of a single hot source delays the inspection, since the peak of contrast will occur 100 s latter when compared with outer and mid thickness defects, precluding the detection of the three defects at the same time.

Meanwhile, DATT enables the detection of the three defects at the same time, at 55 s when the two power sources are applied simultaneously, as depicted in **Fig. 8** the correspondent surface temperature profile.

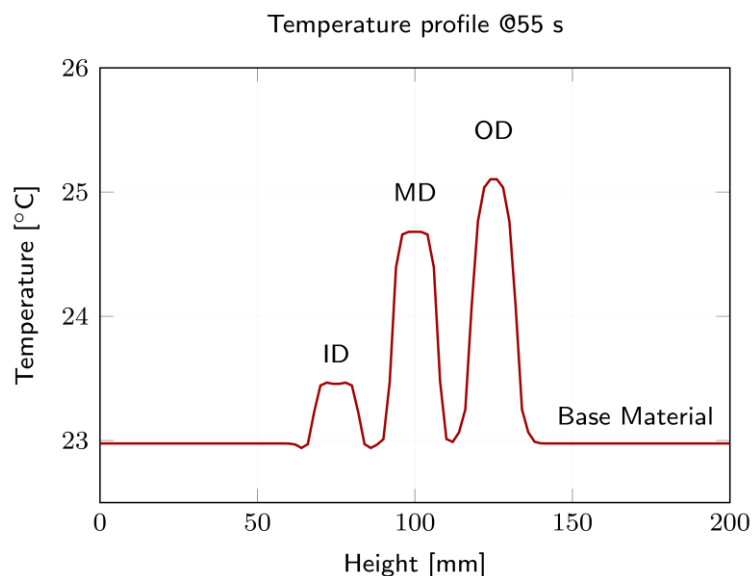


Fig. 8. Temperature profile in the outer wall surface at 55 s (Heat and Cold): the three defects are visible.

In **Fig. 9** are plotted the temperature distribution through the thickness for selected frames when the maximum contrasts occur of the mid thickness defect using DATT versus ATT. It is visible that the contrast gain of 141% for the detection of the mid thickness defect is explained with the increase of the temperature gradient from the surface to mid thickness.

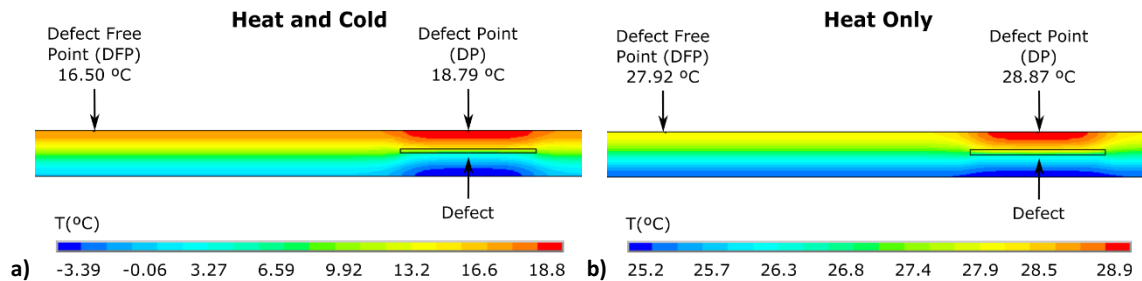


Fig. 9. Numerical results: detailed view of temperature distributions for the mid thickness defect at the instant of maximum contrast: a) DATT achieves 2.29 °C contrast at 83 s; b) ATT achieves 0.94 °C contrast at 75 s.

4.2. Experimental validation results

4.2.1. Coolant fluid

From each test, a thermographic video was made where the evolution of the sample surface temperature was monitored. A few points were defined in the thermographic video which corresponded to the location of the defects and its neighbour area. For each frame, the points over each defect were subtracted by the mean of the neighbour points obtaining the contrast for each moment. Then, using these values, a contrast temperature chart was built, where the evolution of the temperature contrast throughout each experiment, and for each defect, can be seen, as shown in **Fig. 10**.

As depicted in **Fig. 10**, the OD inspection does not seem to benefit from the introduction of cold, as the maximum contrast remains close to 11 °C and occurs always after the heating source is turned off. The same cannot be concluded for the MD, in which the maximum contrast is duplicated, from 2 °C to 4 °C, comparing with heat only or cold only. "Cold then heat" experiment revealed a maximum contrast slightly sooner, 5 to 10 s, than the rest as predicted by the simulation in **Fig. 5**. The ID detection is greatly improved when using the hot and cold sources at the same time, obtaining a contrast change 5 times greater against the heat only technique. However, this contrast increase is mainly due to the cold source being applied to the surface closer to this defect. As seen in **Fig. 10c** using a cold source only in the other surface also improves the result contrast by 4 times. That said, the DATT technique, for this kind of defect, increases the contrast around 25% when compared to "Cold only" experiment.

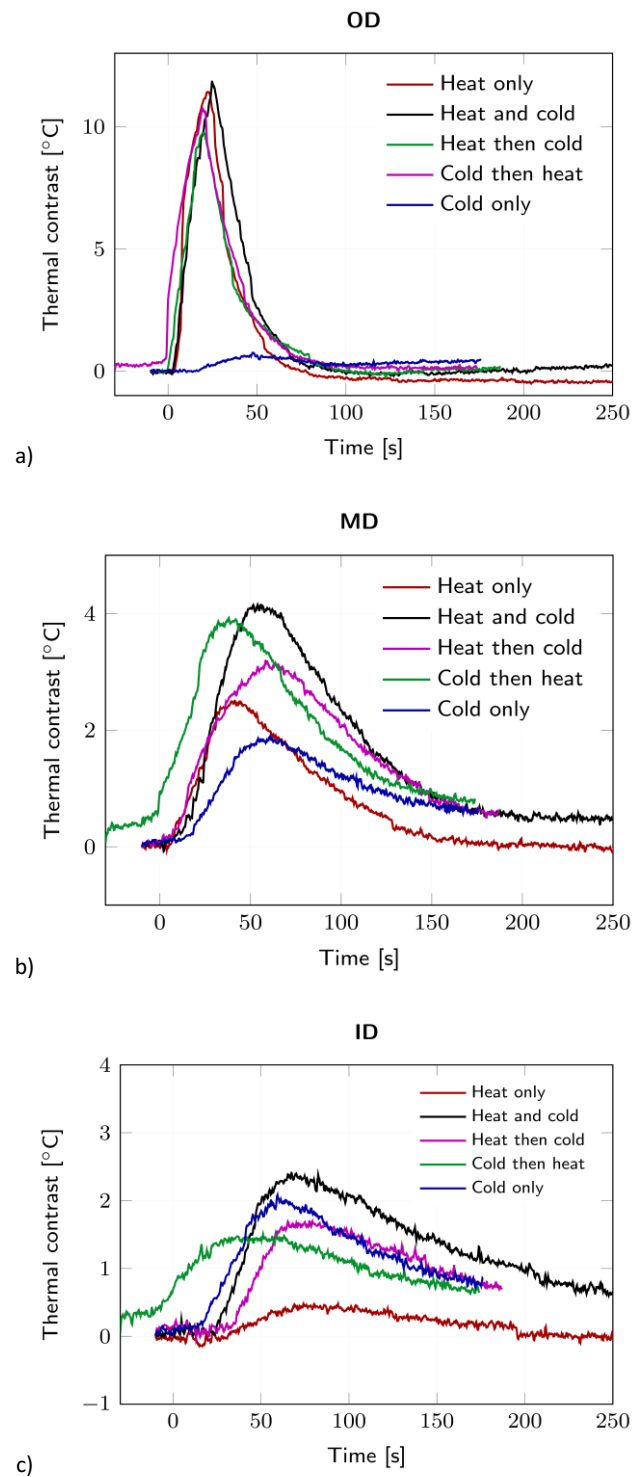


Fig. 10. Experimental temperature contrasts comparison for each defect using the coolant fluid as cold source. The MD inspection benefited with the use of the two sources.

In **Fig. 11** are depicted three thermograms which correspond to the experiment where the heat and cold source were used simultaneously. The first thermogram corresponds to the instant for which the contrast is maximum for the OD and the second to the maximum contrast for the MD. The last thermogram corresponds to the instant the temperature contrasts of both MD and ID are the same.

These times can be easily identified in **Fig. 10**. As expected, the first defect to show up is the OD which is closer to the surface. Then appears the MD and afterwards the ID since the measured surface is furthest away from them.

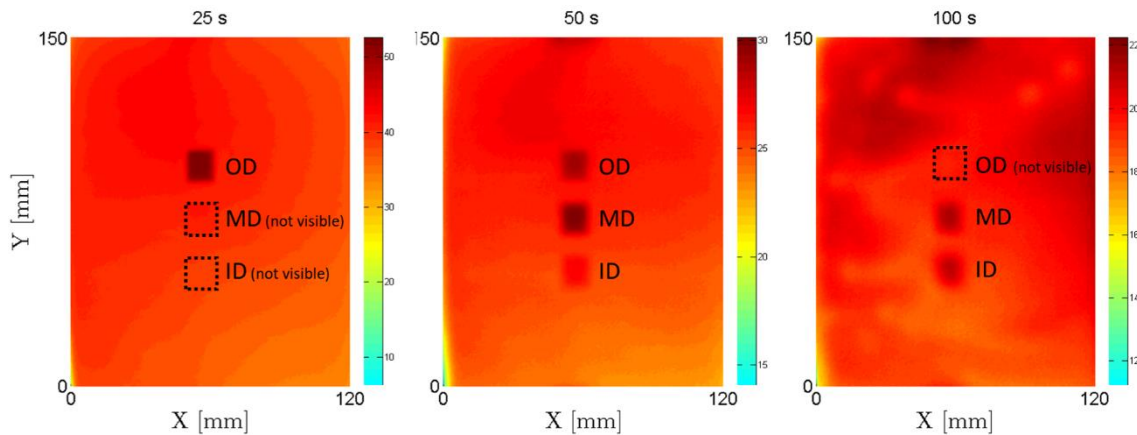


Fig. 11. Experimental thermograms at different instants for the Heat and Cold test (simultaneously).

Fig. 10 allowed to understand that the advantage of the DATT technique is most significant for defects that are not closer to a specific surface hence why, the use of the second sample with 15 mm thickness with only a mid-thickness defect.

Fig. 12 depicts the temperature contrast variation throughout the time with the different settings from **Table 2**. As shown, the contrast increases roughly 50% when using the two sources comparing to one source only. However, does not seem to be very relevant which source comes first.

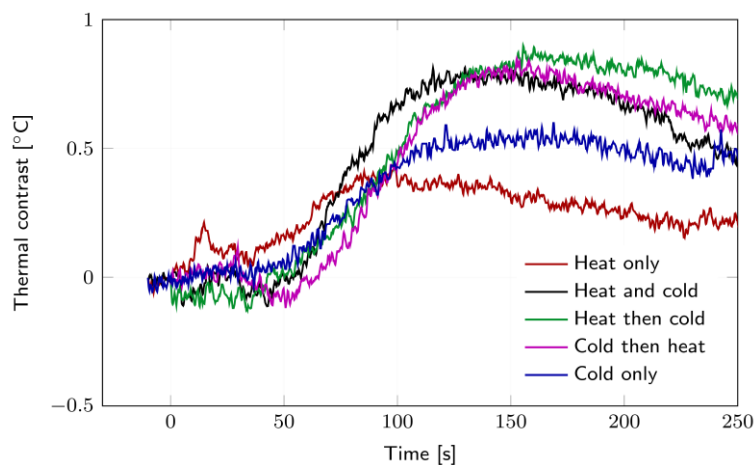


Fig. 12. Experimental temperature contrast variation throughout the time on a 15 mm thickness sample with a defect in mid thickness (15 mm square void 0.5 mm thick).

4.2.1. Cooled air

As mentioned before, the use of a cold air stream is more suitable for an industrial setting although the lower cooling power when compared to the coolant fluid. As happened with the coolant fluid, the OD presented a greater contrast compared to the other defect as long as there is a heat source. The maximum contrast also happens later the farthest the defect is from the measured sample surface. In the "cold only" setup, it is possible to observe that the contrasts obtained are low which is due to the weak cooling power of the vortex. However, in **Fig. 13** it is possible to observe that the MD obtains a small increase in the contrast when employing both the heat and cold source rather than just heat of cold. Envisaging an industrial application several parallel vortex tubes cooling, operating simultaneously, may be used to increase the cooling power and to increase the cooling inspection area. The DATT is based on the same physical phenomena as conventional thermography is. Therefore, the same materials should be suitable for DAAT variant.

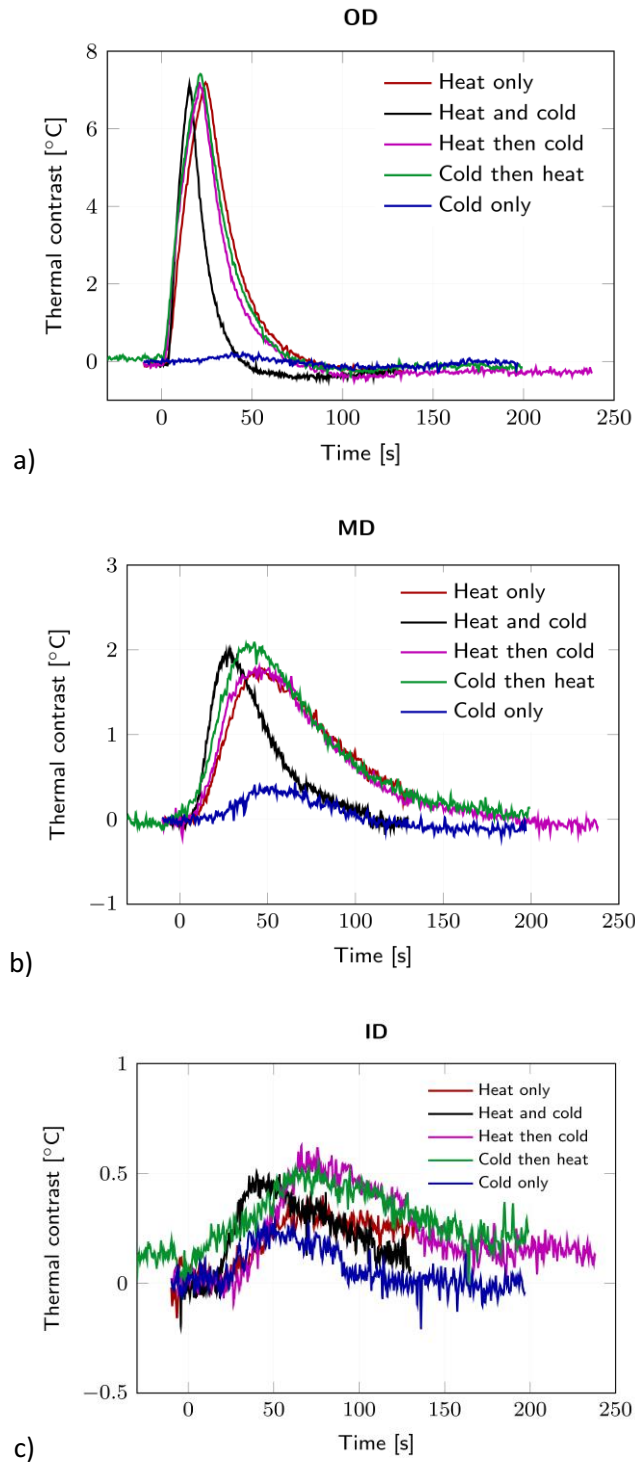


Fig. 13. Temperature contrasts comparison for each defect using the air as cold source. The MD detection benefited with the use of the two sources.

5. Conclusions

In this paper, it was presented an innovative variant of the Active Transient Thermography (ATT), designated Double Active Transient Thermography (DATT), in order to increase the temperature contrast, for delamination defects at different depths and locations.

- The temperature gradient throughout the thickness, which is not possible to measure experimentally, was investigated using numerical simulation, recognising that there is indeed an advantage in using a hot and a cold power source in each surface of the inspected part;
- The experimental tests corroborate the results of the contrasts obtained numerically, revealing that DATT is particularly interesting for mid thickness defects. For the experiments conducted to validate DATT, the contrast obtained was 2 times greater than the contrast obtained with ATT;
- For defects closer to the cold source, the temperature contrast can increase up to the double when comparing to using one heat source only. However, when comparing to using only a cold source over the surface closer to the defect, the contrast gain is marginal, up to 20%;
- Although with the cold air source the contrasts results achieved are not as good as those obtained with cooling liquid, it was demonstrated that it can benefit the inspection process.

Acknowledgements

Authors gratefully acknowledge the funding of Project POCI-01-0145-FEDER-016414 (FIBR3D), cofinanced by Programa Operacional Competitividade e Internacionalização and Programa Operacional Regional de Lisboa, through Fundo Europeu de Desenvolvimento Regional (FEDER) and by National Funds through Fundação para a Ciência e a Tecnologia (FCT - MCTES). MAM, MSC and TGS acknowledge FCT - MCTES for its financial support via the project UIDB/00667/2020 (UNIDEMI).

References

- [1] Santos TG, Oliveira JP, Machado MA, Inácio PL, Duarte VR, Rodrigues TA, et al. Reliability and NDT Methods, 2020, p. 265–95. https://doi.org/10.1007/978-3-030-44522-5_8.
- [2] Ciampa F, Mahmoodi P, Pinto F, Meo M. Recent Advances in Active Infrared Thermography for Non-Destructive Testing of Aerospace Components. *Sensors* 2018;18:609. <https://doi.org/10.3390/s18020609>.
- [3] Quan Z, Wu A, Keefe M, Qin X, Yu J, Suhr J, et al. Additive manufacturing of multi-directional preforms for composites: opportunities and challenges. *Mater Today* 2015;18:503–12. <https://doi.org/10.1016/j.mattod.2015.05.001>.
- [4] Carvalho MS, Martins AP, Santos TG. Simulation and validation of thermography inspection for components produced by additive manufacturing. *Appl Therm Eng* 2019;159:113872. <https://doi.org/10.1016/j.applthermaleng.2019.113872>.
- [5] Machado MA, Antin K-N, Rosado LS, Vilaça P, Santos TG. High-speed inspection of delamination defects in unidirectional CFRP by non-contact eddy current testing. *Compos Part B Eng* 2021;224:109167. <https://doi.org/10.1016/j.compositesb.2021.109167>.
- [6] Machado MA, Rosado L, Pedrosa N, Miranda RM, Piedade M, Santos TG. Customized Eddy Current Probes for Pipe Inspection. *Stud Appl Electromagn Mech* 2017;42:283–90. <https://doi.org/10.3233/978-1-61499-767-2-283>.
- [7] Duarte VR, Rodrigues TA, Machado MA, Pragana JPM, Pombinha P, Coutinho L, et al. Benchmarking of Nondestructive Testing for Additive Manufacturing. *3D Print Addit Manuf* 2021;8:263–70. <https://doi.org/10.1089/3dp.2020.0204>.
- [8] Machado MA, Inácio PL, Santos RA, Gomes AF, Martins AP, Carvalho MS, et al. Inspection of composite parts produced by additive manufacturing: Air-coupled ultrasound and thermography. *58th Annu. Conf. Br. Inst. Non-Destructive Testing, NDT 2019*, Telford, UK: 2019.
- [9] Costa FB, Machado MA, Bonfait GJ, Vieira P, Santos TG. Continuous wave terahertz

- imaging for NDT: Fundamentals and experimental validation. *Measurement* 2021;172:108904. <https://doi.org/10.1016/j.measurement.2020.108904>.
- [10] Vavilov VP. Modeling thermal NDT problems. *Int J Heat Mass Transf* 2014;72:75–86. <https://doi.org/10.1016/j.ijheatmasstransfer.2013.12.084>.
- [11] Lei L, Bortolin A, Bison P, Maldague X. Detection of insulation flaws and thermal bridges in insulated truck box panels. *Quant Infrared Thermogr J* 2017;14:275–84. <https://doi.org/10.1080/17686733.2017.1336899>.
- [12] Lei L, Ferrarini G, Bortolin A, Cadelano G, Bison P, Maldague X. Thermography is cool: Defect detection using liquid nitrogen as a stimulus. *NDT E Int* 2019;102:137–43. <https://doi.org/10.1016/j.ndteint.2018.11.012>.
- [13] Lizaranzu M, Lario A, Chiminelli A, Amenabar I. Non-destructive testing of composite materials by means of active thermography-based tools. *Infrared Phys Technol* 2015;71:113–20. <https://doi.org/10.1016/j.infrared.2015.02.006>.
- [14] Jolly M, Prabhakar A, Sturzu B, Hollstein K, Singh R, Thomas S, et al. Review of Non-destructive Testing (NDT) Techniques and their Applicability to Thick Walled Composites. *Procedia CIRP* 2015;38:129–36. <https://doi.org/10.1016/j.procir.2015.07.043>.
- [15] Shepard SM, Lhota JR, Ahmed T. Flash thermography contrast model based on IR camera noise characteristics. *Nondestruct Test Eval* 2007;22:113–26. <https://doi.org/10.1080/10589750701448662>.
- [16] Mabrouki F, Genest M, Shi G, Fahr A. Numerical modeling for thermographic inspection of fiber metal laminates. *NDT E Int* 2009;42:581–8. <https://doi.org/10.1016/j.ndteint.2009.02.010>.
- [17] Peeters J, Ibarra-Castanedo C, Sfarra S, Maldague X, Dirckx JJJ, Steenackers G. Robust quantitative depth estimation on CFRP samples using active thermography inspection and numerical simulation updating. *NDT E Int* 2017;87:119–23. <https://doi.org/10.1016/j.ndteint.2017.02.003>.
- [18] Ghadermazi K, Khozeimeh MA, Taheri-Behrooz F, Safizadeh MS. Delamination

- detection in glass–epoxy composites using step-phase thermography (SPT). *Infrared Phys Technol* 2015;72:204–9. <https://doi.org/10.1016/j.infrared.2015.08.006>.
- [19] Peeters J, Ibarra-Castanedo C, Khodayar F, Mokhtari Y, Sfarra S, Zhang H, et al. Optimised dynamic line scan thermographic detection of CFRP inserts using FE updating and POD analysis. *NDT E Int* 2018;93:141–9. <https://doi.org/10.1016/j.ndteint.2017.10.006>.
- [20] Pastuszak PD. Characterization of Defects in Curved Composite Structures Using Active Infrared Thermography. *Procedia Eng* 2016;157:325–32. <https://doi.org/10.1016/j.proeng.2016.08.373>.
- [21] Grosso M, Lopez JEC, Silva VMA, Soares SD, Rebello JMA, Pereira GR. Pulsed thermography inspection of adhesive composite joints: computational simulation model and experimental validation. *Compos Part B Eng* 2016;106:1–9. <https://doi.org/10.1016/j.compositesb.2016.09.011>.
- [22] Swiderski W. Non-Destructive Testing of Carbon Fiber Reinforced Plastic by Infrared Thermography Methods 2016;10:1470–3. <https://doi.org/10.5281/zenodo.1128165>.
- [23] Yi Q, Tian GY, Malekmohammadi H, Zhu J, Laureti S, Ricci M. New features for delamination depth evaluation in carbon fiber reinforced plastic materials using eddy current pulse-compression thermography. *NDT E Int* 2019;102:264–73. <https://doi.org/10.1016/j.ndteint.2018.12.010>.
- [24] Liu Y, Wu J-Y, Liu K, Wen H-L, Yao Y, Sfarra S, et al. Independent component thermography for non-destructive testing of defects in polymer composites. *Meas Sci Technol* 2019;30:044006. <https://doi.org/10.1088/1361-6501/ab02db>.
- [25] Wu S, Gao B, Yang Y, Zhu Y, Burrascano P, Laureti S, et al. Halogen optical referred pulse-compression thermography for defect detection of CFRP. *Infrared Phys Technol* 2019;102:103006. <https://doi.org/10.1016/j.infrared.2019.103006>.
- [26] Belhabib S, Zhang W, Guessasma S, Nouri H, Zhu J. Challenges of additive manufacturing technologies from an optimisation perspective. *Int J Simul Multidiscip Des Optim* 2016;6:A9. <https://doi.org/10.1051/smdo/2016001>.

- [27] Es-Said OS, Foyos J, Noorani R, Mendelson M, Marloth R, Pregger BA. Effect of Layer Orientation on Mechanical Properties of Rapid Prototyped Samples. *Mater Manuf Process* 2000;15:107–22. <https://doi.org/10.1080/10426910008912976>.